water

MDPI

Article

Preparation of CTAB-ATP/CTS Composite Adsorbent and Removal Performance of Norfloxacin in Water

Hongxia Du [1], Zihan Wang [2], Kinjal J. Shah [2,*] and Yongjun Sun [2,*]

[1] School of Chemical and Material Engineering, Nanjing Polytechnic Institute, Nanjing 210048, China; hxdu@mail.ustc.edu.cn
[2] College of Urban Construction, Nanjing Tech University, Nanjing 211816, China
* Correspondence: kjshah@njtech.edu.cn (K.J.S.); sunyongjun@njtech.edu.cn (Y.S.)

Abstract: In this article, attapulgite (ATP) as a raw material, hexadecyltrimethylammonium bromide (CTAB) as a modifier, and chitosan (CTS) as a composite are used to prepare a natural mineral-based composite adsorbent CTAB-ATP/CTS for the adsorption of norfloxacin in water. Scanning electron microscopy (SEM), Fourier transform infrared spectroscopy (FTIR), X-ray diffraction (XRD), and specific surface area (BET) were used for characterization. When the initial pH is 7, the dosage of adsorbent is 3 g/L, and the initial concentration of norfloxacin is 50 mg/L, the reaction temperature is 25 °C, the shaking time is 4 h, and the maximum removal rate and adsorption capacity of CTAB-ATP/CTS for norfloxacin reached 94.62% and 23.66 mg/g, respectively. The adsorption of norfloxacin by CTAB-ATP/CTS is more consistent with the pseudo-second-order kinetic model (R^2 = 0.9999, 0.9998, 0.9999 at initial concentrations of 25 mg/L, 50 mg/L, 75 mg/L), and the Langmuir isotherm adsorption model(R^2 = 0.9903, 0.9935, 0.9933 at temperatures of 25 °C, 30 °C, 35 °C), indicating that the adsorption process of the composite material is controlled by chemical adsorption and its adsorption behavior is mainly single-layer adsorption.

Keywords: attapulgite; hexadecyltrimethylammonium bromide; chitosan; adsorption; norfloxacin

Citation: Du, H.; Wang, Z.; Shah, K.J.; Sun, Y. Preparation of CTAB-ATP/CTS Composite Adsorbent and Removal Performance of Norfloxacin in Water. *Water* **2024**, *16*, 2446. https://doi.org/10.3390/w16172446

Academic Editors: Gongduan Fan and Farzaneh Mahmoudi

Received: 12 June 2024
Revised: 30 July 2024
Accepted: 27 August 2024
Published: 29 August 2024

1. Introduction

Fluoroquinolones (FQs) are broad-spectrum antibiotics that inhibit cell division by efficiently and specifically interfering with DNA rotamase activity [1]. Norfloxacin (NOR) is a fluoroquinolone with excellent broad-spectrum antimicrobial activity and rapid bactericidal activity, which is widely used in the fields of medicine, animal husbandry, and aquaculture [2]. However, about 70% of the NOR cannot be absorbed and enters the water body via human or animal metabolism and is re-accumulated via the food chain, which leads to a persistence phenomenon at low concentrations in the water body [3]. Due to its high emission rate and slow degradation, it has been frequently detected in surface waters, soils, and other sedimentary environments in recent years [4]. NOR residues in water and soil can lead to pathogenic microbial resistance, cause teratogenicity and genotoxicity, and pose a potential threat to organisms and ecosystems [5]. To solve the current challenge of increasing antibiotic detection concentration, effective antibiotic removal methods have also become a research focus. Therefore, studying efficient water treatment techniques to remove antibiotics from wastewater is of great importance for protecting the health of aquatic organisms and ensuring the safety of the aquatic environment and ecosystem.

Research domestically and internationally has shown that commonly used methods for removing quinolone antibiotics include biodegradation [6], advanced oxidation process [7], membrane filtration [8], and adsorption [9]. Biodegradation is the use of microbial degradation metabolism to treat wastewater by artificially creating an environment suitable for microbial proliferation in order to increase the efficiency of the decomposition of organic matter. However, due to the stable chemical structure and bacteriostatic properties of quinolone antibiotics, it is difficult to completely degrade such pollutants through

biodegradation, and prolonged exposure during treatment may lead to the gradual accumulation of resistance in bacteria and ultimately lead to the emergence of new pollutant resistance genes [10]. The advanced oxidation process for treating antibiotic wastewater mainly includes photocatalytic technology [11], Fenton oxidation technology [12], and ozone oxidation technology [13] and other processes. Although the advanced oxidation method for removing quinolone antibiotics is obvious, the treatment cost is still high, the operation of the equipment requires high conditions, and the treatment process is often a reaction of by-products, resulting in secondary pollution and meaning the toxicity of the degraded chemical products needs to be investigated alongside other problems [14]. The membrane filtration has the disadvantages of easy contamination of the filter membrane, low stability, and limited range [15]. Compared to other techniques, adsorption is usually simple, efficient, economically feasible, and applicable to a wide concentration range, and therefore represents one of the most important methods for the removal of antibiotics in the aqueous environment [16].

At present, adsorption technology has problems such as low adsorption capacity or long adsorption time, and the adsorbent loaded with metal ions tends to release the metal ions back into the environment, resulting in secondary pollution. Therefore, developing an environmentally friendly adsorbent that can quickly remove environmental pollutants on a large scale is the key to the development of adsorption technology [17]. In recent years, environmentally friendly natural mineral-based adsorbents have received great attention from researchers due to their low pollution potential, strong regenerative ability, numerous active functional groups, and easy graft modification [18]. Among them, attapulgite (ATP) has attracted much attention due to its large specific surface area, large porosity, environmental friendliness, low cost, non-toxicity, and good adsorption performance [19]. However, the adsorption capacity of ATP for certain pollutants is limited, and studies have shown that the adsorption effect was significantly improved by modifying it to achieve effective adsorption of organic pollutants [20]. Using organic surfactants as modifiers, high molecular weight organic groups were used to replace the exchangeable cations between the aconite layers as well as part of the crystal water and adsorbed water in the lattice, thereby changing the surface functional groups, increasing the distance between layers, and improving at the same time the hydrophobicity, which improves the adsorption capacity and selectivity of aconite [21]. Meanwhile, the use of chitosan (CTS), a natural polymer, as an adsorbent for wastewater treatment has attracted great attention due to its excellent adsorption capacity, low cost, biodegradability, and non-toxicity [22]. Its biodegradability means that it does not persist in the environment for long periods of time, thus reducing potential hazards to the environment and the human body. Its molecules contain a large number of reactive groups -OH-NH_2, which help to reduce the properties of ATP such as strong swelling and suspension in wastewater, and improve the ability to adsorb organic matter [23].

On this basis, in this experiment, hexadecyltrimethylammonium bromide (CTAB) was selected to modify the acid-activated natural mineral attapulgite (ATP), and then it was assembled with chitosan (CTS) using the acid dissolution ultrasonic method to obtain a green composite adsorbent CTAB-ATP/CTS. During the preparation process of the composite experiment, the effects of acetic acid concentration, ultrasonication time, and CTAB-ATP:CTS composite mass ratio on the adsorption performance of the composite adsorbent were investigated. The physicochemical properties were investigated using SEM, FTIR, XRD, and BET. The effects of initial pH, adsorbent dose, and initial norfloxacin concentration on the removal of norfloxacin by adsorption were also studied. Finally, the adsorption mechanism was investigated using a pseudo-first-order kinetic model, a pseudo-second-order kinetic model, and an intraparticle diffusion model, an isothermal Freundlich model, and an isothermal Langmiur model, respectively.

2. Materials and Methods

2.1. Materials

Attapulgite (ATP) was purchased from Changzhou Dingbang Mineral Products Technology Co., Ltd., Changzhou, China Chitosan (CTS) and silver nitrate ($AgNO_3$) were purchased from Shanghai Aladdin Biochemical Technology Co., Ltd., Shanghai, China. Hexadecyltrimethylammonium bromide ($C_{19}H_{42}BrN$) and norfloxacin ($C_{16}H_{18}FN_3O_3$) were purchased from Shanghai McLean Biochemical Technology Co., Ltd., Shanghai, China. Acetic acid ($C_2H_4O_2$), anhydrous ethanol (C_2H_6O), sodium hydroxide (NaOH) were purchased from Sinopharm Chemical Reagent Co., Ltd., Shanghai, China. Hydrochloric acid (HCl) was purchased from Shanghai Lingfeng Chemical Reagent Co., Ltd., Shanghai, China. The above chemicals are analytical reagents.

2.2. Preparation of CTAB-ATP/CTS Adsorbents

First, take the original attapulgite, add a large amount of distilled water, stir evenly, wash for 10 min, filter to remove insoluble impurities and dirt, and finally put it in one electric hot air drying oven (DHG-9070A, Shanghai Jinghong, Shanghai, China) and let dry for 2 h at 80 °C. Finally, grind and pass through a 200 mesh sieve. Then, mix 10 g of attapulgite with 120 mL of 8% mass acetic acid solution and incubate for 2 h in a constant temperature (25 °C) shaking water tank (DKZ-2, Shanghai Jinghong, Shanghai, China). Finally, wash with distilled water until the pH is neutral. The filtered solid is dried in an oven at 80 °C for 2 h and finally ground and passed through a 200 mesh sieve to obtain acetic acid modified attapulgite.

Weigh 0.8 g of cetyltrimethylammonium bromide (CTAB), add 80 mL of anhydrous ethanol to dissolve completely, and add 8.0 g of ATP acetate as purified as above. Ultrasonically modify in an ultrasonic cleaner (G-010S, Shenzhen Gonergy Cleaning Equipments Co., Ltd., Shenzhen, China) at 25 °C for 2 h. After filtration, wash the filter cake until the bromide ions disappear (with 0.01 mol/L $AgNO_3$ solution measurement). Dry at 80 °C for 2 h. After grinding, it pass it through a 200-mesh sieve and label as CTAB-ATP.

A certain amount of chitosan was put into a beaker and injected with different volume proportions of acetic acid solution to dissolve it thoroughly to obtain a relatively viscous colloidal solution, and then different mass ratios of CTAB-ATP were added into the colloidal solution to soak it completely and to wet and stir into a mixed paste. After ultrasonic dispersion for a certain time, the paste was dried in an oven at 105 °C and then ground and stored, which enabled the composite adsorbent CTAB-ATP/CTS with different composite mass ratios to be obtained. The acidification concentration of acetic acid (3%, 5%, 7%, 9%, 11%, and 13%), the sonication time (5 min, 10 min, 15 min, 20 min, 25 min, and 30 min) and the CTAB-ATP: CTS composite mass ratio (1:0.005, 1:0.01, 1:0.02, 1:0.03, 1:0.04, and 1:0.05) were adjusted, and one of the conditions for the preparation of the composite adsorbent was varied.

2.3. Characterisation of CTAB-ATP/CTS Adsorbents

The surface of ATP, CTAB-ATP/CTS adsorbent before and after adsorption was analysed by scanning electron microscopy (SEM, S-3400N, Hitachi, Tokyo, Japan). The functional groups of ATP, CTAB-ATP/CTS adsorbent before and after adsorption were analysed by infrared spectroscopy (FTIR, 510PFT-IR, Nicolet, Madison, WI, USA). The crystal structure of ATP, CTAB-ATP/CTS adsorbent before and after adsorption was determined by X-ray diffraction (XRD, D&advance, Bruker, Germany). The pore size and surface area of ATP, CTAB-ATP/CTS adsorbent before and after adsorption were determined by pore size and specific surface area analysis (BET, Novawin 1994–2016, Quantachrome, Boynton Beach, FL, USA).

2.4. Adsorption Experiments

Weigh 0.1 g of norfloxacin dissolved in 1 L of water to obtain a 100 mg/L norfloxacin stock solution, disperse with ultrasound for a specified time to aid dissolution, and take

40 mL of the known concentration of a norfloxacin solution in a 50 mL Erlenmeyer flask. Close the flask with a stopper, adjust to a certain pH value, then add a certain amount of adsorbent, mix well and place in an electrothermal, thermostatic shaking water bath at a speed of 120 rpm. Set at 25, remove the Erlenmeyer flask by shaking for 1 min. Give it over a period of time, let it stand for some time, and then extract the supernatant. The sample should be filtered with a 0.45 m filter membrane and then measured under the ultraviolet spectrophotometer (UV-5500PC, Shanghai Yuananalytical Instrument Co., Ltd., Shanghai, China) at a wavelength of 273 nm. The standard curve of norfloxacin is shown in Figure S1. The removal rate of norfloxacin by the adsorbent and the static adsorption capacity can be calculated by Equations (1) and (2), respectively.

$$Q = \frac{C_0 - C_t}{C_0} \times 100\% \quad (1)$$

$$q_e = \frac{V_0(C_0 - C_t)}{m} \quad (2)$$

where, C_0 is the initial concentration of norfloxacin in solution, mg/L; C_t is the concentration of norfloxacin in solution after adsorption, mg/L; V_0 is the volume of solution, L; m is the dosage of adsorbent in solution, g.

The initial concentration of norfloxacin was set at 25 mg/L, 50 mg/L, and 75 mg/L under the conditions of initial pH 7, adsorbent dosage of 3 g/L, and adsorption temperature of 25 °C, and was shaken in an electrically heated thermostatic oscillating water bath at the speed of 120 r/min for 5, 10, 20, 40, 60, 90, 120, 180, 240, 300, and 360 min. Pseudo-first-order kinetic (3), pseudo-second-order kinetic (4), intra-particle diffusion (5) were used to fit the experimental data, and their equations were expressed as:

$$\lg(q_e - q_t) = lgq_e - k_1 t \quad (3)$$

$$\frac{t}{q_t} = \frac{1}{k_2 q_e^2} + \frac{t}{q_e} \quad (4)$$

$$q_t = k_{ip} t^{\frac{1}{2}} + C \quad (5)$$

where, q_e is the adsorption capacity of norfloxacin at equilibrium, mg/g; q_t is the adsorption capacity of norfloxacin at t, mg/g; t is the adsorption time, min; k_1 is the pseudo-first-order kinetic adsorption rate constant, min^{-1}; k_2 is the pseudo-second-order kinetic adsorption rate constant, $g \cdot mg^{-1} \cdot min^{-1}$; k_{ip} is the intra-particle diffusion constant, $mg \cdot g^{-1} \cdot min^{-0.5}$; C is a constant related to the thickness of the boundary layer, mg/g.

Norfloxacin solutions with concentrations of 10 mg/L, 15 mg/L, 20 mg/L, 25 mg/L, 50 mg/L, 75 mg/L, and 100 mg/L were taken and adsorbed by cyclonic oscillation at a rate of 120 r/min at temperatures of 25 °C, 30 °C, and 35 °C for 4 h at an initial pH of 7 and adsorbent dosing of 3 g/L. The data was simulated in the isotherm curve using the Langmuir (6) and Freundlich (7) isotherm adsorption models, and their equations are represented as follows:

$$q_e = \frac{K_L q_m C_e}{1 + K_L C_e} \quad (6)$$

$$q_e = K_F + C_e^{\frac{1}{n}} \quad (7)$$

where, q_e is the adsorption capacity of norfloxacin at equilibrium, mg/g; q_m is the maximum adsorbed amount of norfloxacin, mg/g; C_e is the concentration of norfloxacin in the solution at equilibrium, mg/L; K_L is the Langmiur adsorption equilibrium constant, which correlates with adsorption energy, L/mg; K_F is the Freundlich adsorption equilibrium constant, which correlates with adsorption energy, mg/g; n is the constant related to adsorption energy.

3. Results and Discussion

3.1. Optimisation of CTAB-ATP/CTS Preparation Conditions

As shown in Figure 1a, the removal rate and adsorption capacity of the adsorbent for norfloxacin showed an overall increasing trend with an increasing acetic acid concentration, and the best effect was obtained at an acetic acid concentration of 9%, where the removal rate of norfloxacin is 75.97% and the adsorption capacity is 18.99 mg/g. This was attributed to the fact that proper acid treatment caused a change in the morphology of the ATP surface, resulting in a more loosely packed interlamellar structure of ATP intercalation type. The chitosan is favorably complexed on the surface of aconite, thereby increasing the adsorption capacity [24]. The adsorption of norfloxacin by the adsorbent was subsequently reduced when the acetic acid concentration was higher than 9%.

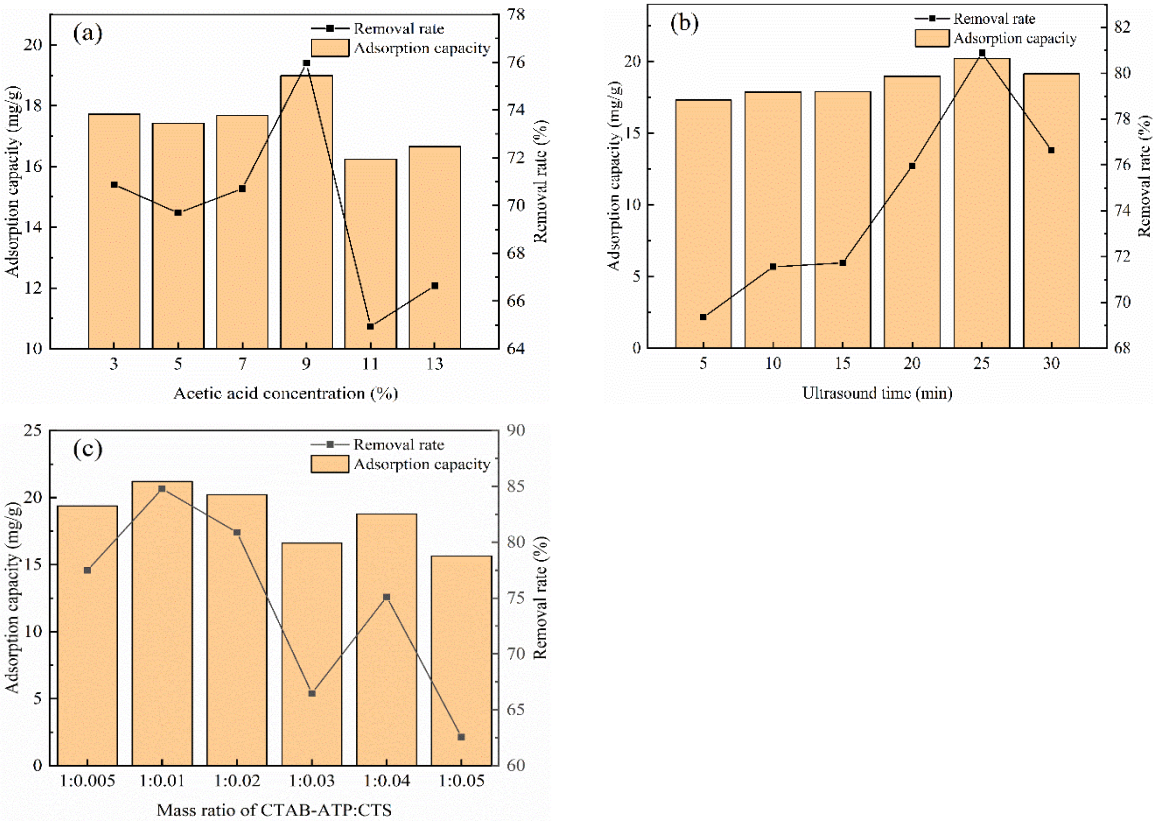

Figure 1. Optimisation of CTAB-ATP/CTS preparation conditions: effect of (**a**) acetic acid concentration; (**b**) sonication time; (**c**) CTAB-ATP:CTS mass ratio. Note: adsorbent adsorption conditions: adsorbent dosage: 2 g/L; initial concentration of norfloxacin: 50 mg/L; volume of norfloxacin solution: 40 mL; adsorption time: 4 h.

As shown in Figure 1b, the removal rate and adsorption capacity of the CTAB-ATP/CTS composite adsorbent on norfloxacin showed a general trend that first increased and then decreased with increasing sonication time, and the adsorption effect on norfloxacin was best when the ultrasound time was 25 min, the removal rate of norfloxacin was 80.89%, and the adsorption capacity was 20.22 mg/g. The adsorption performance of the composite adsorbent on norfloxacin decreased when the ultrasound time was more than 25 min. Ultrasonic dispersion can increase the flux of chitosan molecules, improve the interlayer domain of bumpy clay, promote the diffusion of chitosan molecules and effective loading of bumpy clay, and improve the adsorption performance [25]. After reaching a certain level, continued ultrasonication leads to uneven loading of chitosan on the surface of uneven clay, and repeated loading leads to loss of active sites and weaker adsorption performance.

As shown in Figure 1c, the removal and adsorption of norfloxacin by the adsorbent were 77.49% and 19.37 mg/g, respectively, when the composite mass ratio was 1:0.005. When the loading of chitosan was increased to a composite mass ratio of 1:0.01, the removal and adsorption of norfloxacin by the adsorbent were significantly increased and reached the optimum, which were 84.79% and 21.20 mg/g, respectively. However, as the loading of chitosan further increased, the removal rate and adsorption of norfloxacin decreased. This may be due to the fact that the adsorption capacity of CTAB-ATP/CTS composites is related to the amount of chitosan that effectively penetrates into the interlayer of bumpy soil [26]. When the amount of chitosan in the solution exceeded the cation exchange capacity of the bumpy clay, the excess chitosan could not effectively penetrate into the interlayer of the bumpy clay, but instead accumulated in and around the pores of the bumpy clay, resulting in pore clogging and a decrease in adsorption capacity.

3.2. Characterisation of CTAB-ATP/CTS Adsorbents

As shown in Figure 2a, ATP has a large number of rod-shaped rod crystal structures with relatively well-defined contour lines and a large particle size. Figure 2b shows that CTAB-ATP/CTS is mainly spherical in shape and has relatively smooth edge lines; the particles are more widely distributed, the organization is looser, and many folds and void structures appear random. This indicates that the modifier transformed the original tight stacking of ATP into a relatively loose structure, and the interlayer distance and voids were obviously larger, which favored the adsorption of norfloxacin on the composites. Figure 2c shows that the surface pores of CTAB-ATP/CTS adsorbed with norfloxacin were significantly reduced and developed into highly aggregated agglomerates, which may be due to the fact that norfloxacin had already penetrated into the intermediate layer of CTAB-ATP/CTS.

As shown in Figure 2d, the absorption peaks of concave clay appeared in all three curves. The absorption peaks at 3543 cm^{-1}, 3546 cm^{-1} and 3540 cm^{-1} can be attributed to the hydroxyl group stretching vibration in Al-O-H, the absorption peaks at 1654 cm^{-1}, 1653 cm^{-1}, and 1652 cm^{-1} are the hydroxyl O-H bending vibrations of the water molecules in the interlayer, and the absorption peak at 971 cm^{-1} were the octahedral Si-O-Si stretching vibrations in the ATP lattice [27,28]. The infrared spectra of CTAB-ATP/CTS showed two absorption peaks near 3000–2500 cm^{-1} (2927 cm^{-1} and 2852 cm^{-1}) compared to the original ATP, which could be recognized as -CH-symmetric and anti-symmetric telescopic vibrational absorption peaks [29], which demonstrate the successful complexation of ATP with CTAB and CTS [30]. Compared to native ATP, the C-H symmetric bending peaks before and after adsorption of norfloxacin on CTAB-ATP/CTS were shifted from 1495 cm^{-1} to 1414 cm^{-1} and 1474 cm^{-1}, respectively.

As shown in Figure 2e, all the three samples contained bumpy clay diffraction peaks at $2\theta = 8.49°$, 16.40°, 19.85°, 24.16°, 27.44°, and 35.32° (PDF#31-0783), in addition to impurities such as SiO_2 at $2\theta = 26.64°$, 50.14°, 59.99° (PDF#46-1045) and impurities such as Al_2O_3 (PDF#46-1212) at $2\theta = 37.38°$, 68.20°. The characteristic peaks of ATP did not change when the original ATP was compared with CTAB-ATP/CTS, indicating that the introduction of CTAB and CTS did not change the crystal structure of ATP. The decrease in the intensity of the typical peaks of SiO_2 before and after the adsorption of norfloxacin on CTAB-ATP/CTS suggests that SiO_2 may be involved in the reaction [31].

As shown in Figure 2f–h, the adsorption–desorption isotherms of the three samples showed typical type IV isotherms with obvious H3 hysteresis loops, indicating the mesoporous structure of the adsorbent [32]. The pore distribution curves show that the main pore size distribution of the three samples is 2–15 nm, which also suggests that the adsorption materials are mainly mesoporous structures. In addition, the specific surface and pore structure parameters of the three samples are listed in Table 1. CTAB-ATP/CTS showed an increase in specific surface area from 16.4610 m^2/g to 69.2159 m^2/g and an increase in total void volume, which increased from 0.021969 cm^2/g to 0.141051 cm^2/g compared to ATP. The average pore size decreased slightly, which may be due to the fact that ATP's

water and internal crystals in the interlayer structure. Water from ATP was removed at high temperatures, which exposed the pore channels, thus increasing the pore volume of CTAB-ATP/ CTS, while loading with CTAB and CTS further increased the specific surface area and increased the adsorption capacity. The specific surface area, total void volume, and average pore diameter of the adsorbed CTAB-ATP/CTS were further increased compared to those of the adsorbed CTAB-ATP/CTS. The likely reason for this phenomenon is that the adsorption of norfloxacin on the surface of CTAB-ATP/CTS resulted in the formation of some tiny concave and convex surfaces, which increased the specific surface area.

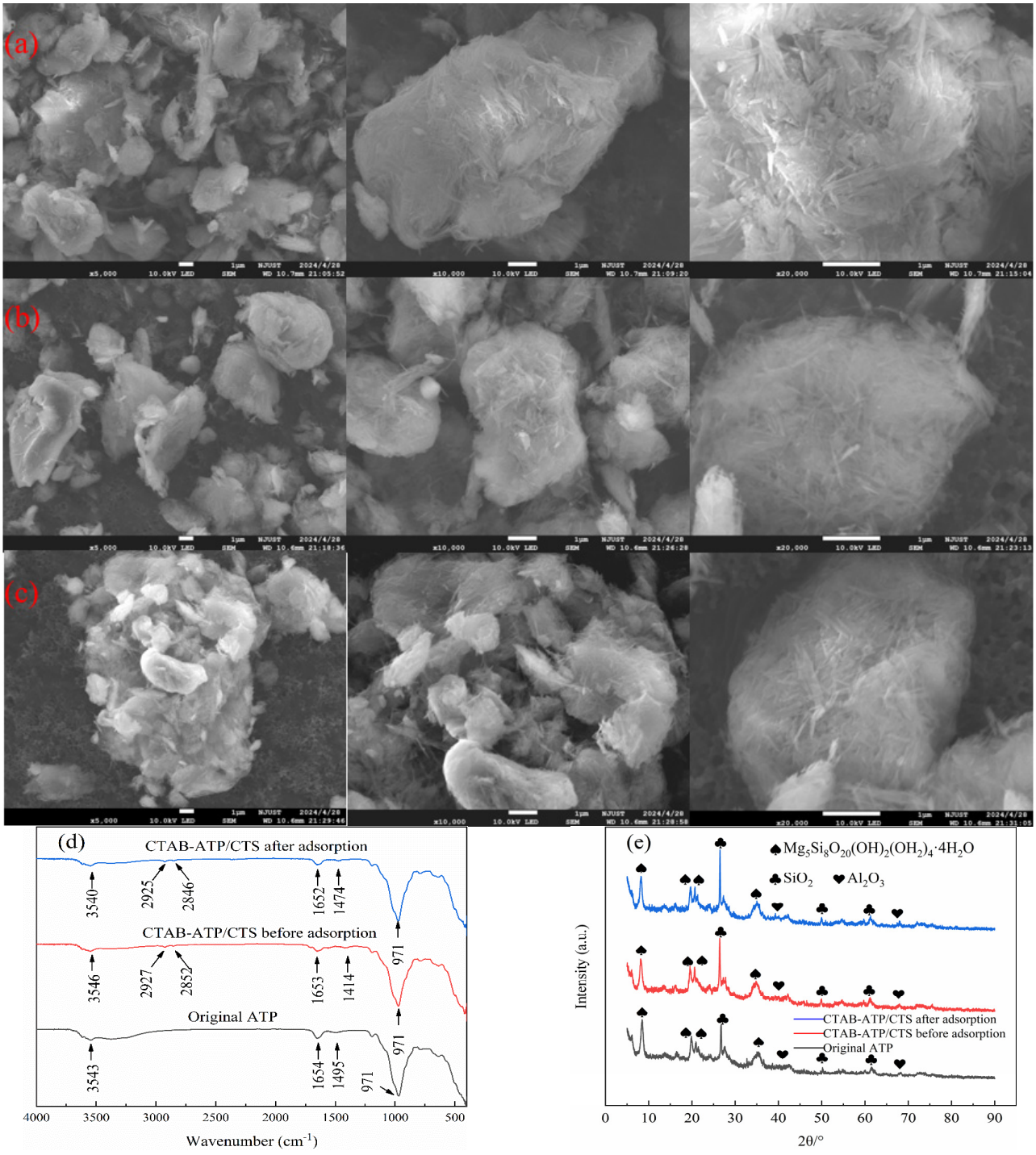

Figure 2. *Cont.*

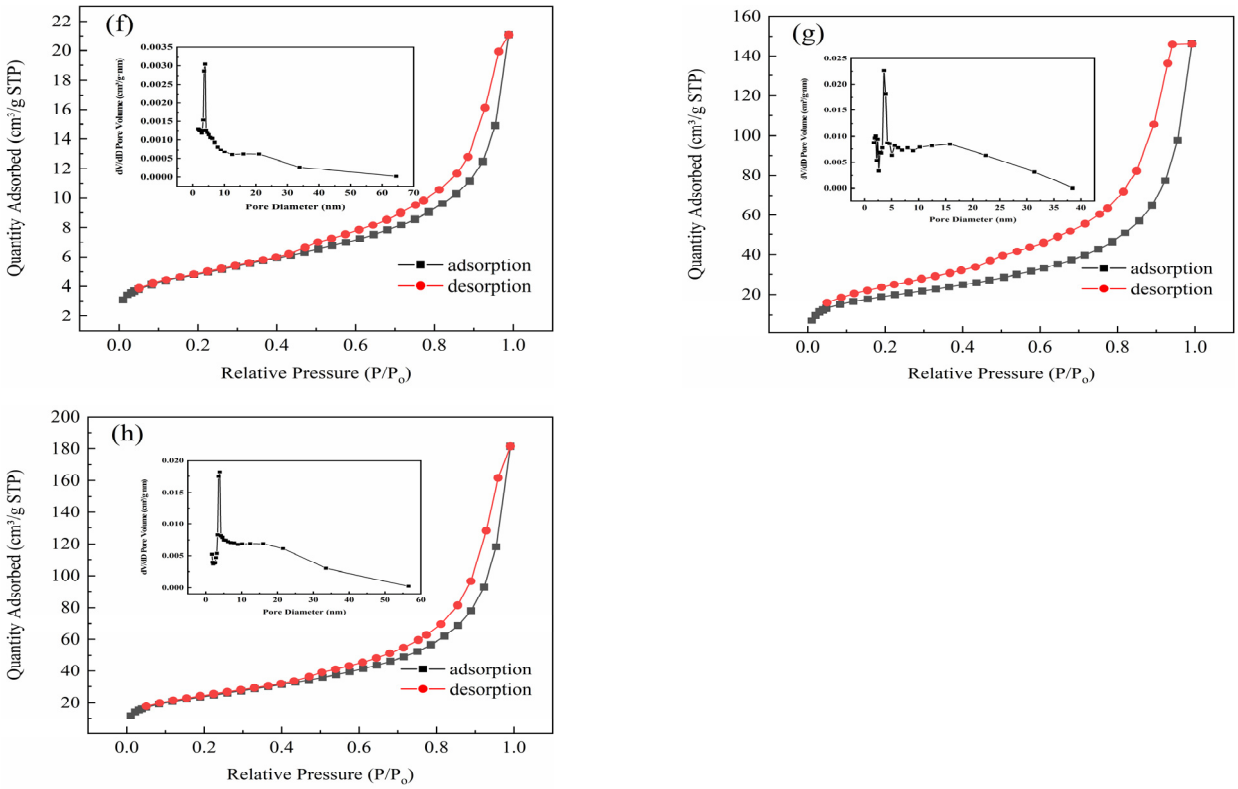

Figure 2. SEM characterisation of (**a**) pro-ATP; (**b**) CTAB-ATP/CTS before adsorption; (**c**) CTAB-ATP/CTS after adsorption; (**d**) FTIR characterisation and (**e**) XRD characterisation of pro-ATP, CTAB-ATP/CTS before and after adsorption; BET characterisation of (**f**) pro-ATP; (**g**) CTAB-ATP/CTS before adsorption; (**h**) CTAB-ATP/CTS after adsorption.

Table 1. Specific surface area and pore structure parameters of ATP, CTAB-ATP/CTS before adsorption and CTAB-ATP/CTS after adsorption.

Sample	Specific Surface Area (m^2/g)	Total Void Volume (cm^2/g)	Average Pore Size (nm)
ATP	16.4610	0.021969	9.3055
CTAB-ATP/CTS before adsorption	69.2159	0.141051	9.1745
CTAB-ATP/CTS after adsorption	86.3373	0.172600	12.2968

3.3. Study of Factors Affecting Adsorption of Norfloxacin by CTAB-ATP/CTS

As shown in Figure 3a, under the same reaction conditions (Initial concentration: 50 mg/L, dosage: 2 g/L, pH: 7), the adsorption of norfloxacin by single chitosan (CTS) and single attapulgite (ATP) was low, and the adsorption of norfloxacin by attapulgite modified with hexadecyltrimethylammonium bromide (CATB-ATP) was greatly improved, with the removal rate and the adsorption capacity of 82.07% and 20.52 mg/g, respectively. The chitosan-loaded composite adsorbent (CTAB-ATP/CTS) showed the best effect on norfloxacin with a removal rate and adsorption capacity of 89.54% and 22.38 mg/g, respectively. Other studied adsorbents for norfloxacin, for example, Li et al. [33] investigated the adsorption capacity of an attapulgite-biochar composites for norfloxacin as 5.24 mg/g (initial concentration: 20 mg/L, dosage: 4 g/L, pH: 6.81); Wu et al. [34] synthesised a novel magnetic molecularly imprinted chitosan/γ-FeO composite with an adsorption capacity of 6.29 mg/g for norfloxacin (initial concentration: 35 mg/L, dosage: 2 g/L, pH: 7). Compared with these adsorbents, the adsorbent prepared in this experiment was characterised by good adsorption effect and low dosage.

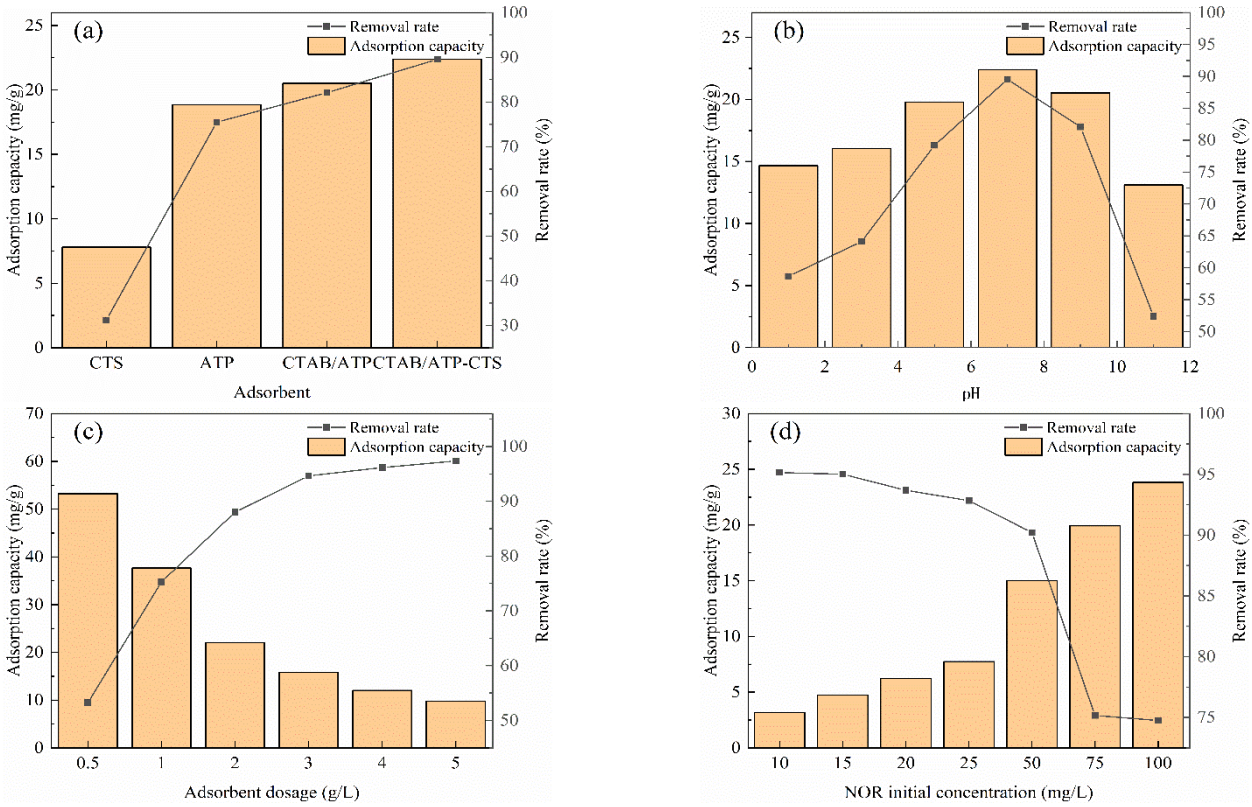

Figure 3. Study of factors affecting adsorption of norfloxacin by CTAB-ATP/CTS: effect of (**a**) selection of adsorbent materials; (**b**) effect of initial pH; (**c**) effect of adsorbent dosage; (**d**) initial norfloxacin concentration. Note: adsorbent preparation conditions: acetic acid concentration: 9%; sonication time: 25 min; CTAB-ATP: CTS mass ratio: 1:0.01.

As shown in Figure 3b, the removal rate and adsorption capacity of the adsorbent for norfloxacin were only 58.67% and 14.67 mg/L at pH 1. Within the range of 1–7, the removal rate and adsorption capacity of the adsorbent for norfloxacin increase with the increase of pH value. The removal rate and adsorption capacity of the composite adsorbent for norfloxacin reached an optimal level at pH 7, which were 89.54% and 22.38 mg/g. With a further increase in pH, the removal and adsorption capacity of the composite adsorbent for norfloxacin decreased significantly and was only 52.39% and 13.10 mg/g when the pH was 11. This is because NOR has two ionization constants of pK_{a1} = 6.2 (carboxyl group) and pK_{a2} = 8.5 (piperazinyl group) [35]. Due to the protonation of the carboxyl and piperazinyl groups, norfloxacin is mainly present in the cationic NOR^+ form in pH $\leq pK_{a1}$, in the amphoteric $NOR^{\pm}$ form in $pK_{a2} \leq$ pH $\leq pK_{a1}$ and in the anionic NOR^- form in pH $\geq pK_{a1}$ [36]. The charge of the surface active site of the adsorbent is significantly affected by the pH of the solution [37], and the adsorption capacity of NOR increases when the pH is increased from 1 to 7 because the negative surface charge of CTAB-ATP/CTS increases dramatically, resulting in an increase in electrostatic attraction. When the pH is greater than 7, the adsorption capacity of NOR decreases with increasing pH, which is probably due to the increase in NOR^- content, which leads to stronger electrostatic repulsion [38]. These results suggest that electrostatic interactions are the main driving force for NOR adsorption by CTAB-ATP/CTS.

As shown in Figure 3c, the removal rate of norfloxacin was only 53.24% when the adsorbent dose was 0.5 g/L. As the dosage of the adsorbent increased, the removal rate of norfloxacin increased significantly, and the removal rate of norfloxacin increased to 94.62% when the dosage was increased to 3 g/L. When the adsorbent dose was further increased, the adsorption removal rate of norfloxacin changed less. When the concentration of norfloxacin in the simulated wastewater is safe and the dosage of the adsorbent is

increased, the total specific surface area of the adsorbent increases accordingly, the active adsorption sites provided by the adsorbent increases, and the adsorption rate increases [39]. When the dosage further increased, the adsorption sites could not be fully utilized and the change in adsorption effect was small. As the dosage of adsorbent increased, the adsorption capacity for norfloxacin decreased continuously because the increase in dosage resulted in the decrease of norfloxacin that can be loaded per unit mass of CTAB/ATP-CTS, so the adsorption capacity showed a decreasing trend.

As shown in Figure 3d, the removal rate and adsorption capacity of the adsorbent for norfloxacin were 95.15% and 4.76 mg/g, respectively, when the initial norfloxacin concentration was 10 mg/L. When the initial concentration of norfloxacin was increased to 100 mg/L, the removal rate of the adsorbent for norfloxacin decreased to 71.45% and the capacity of the adsorbent increased to 35.72 mg/g. The results showed that the initial concentration was negatively correlated with the removal rate and positively correlated with the adsorption capacity. The concentration correlated negatively with norfloxacin removal and positively with adsorption capacity. This is because for the same dose of adsorbent, the adsorption sites are approximately the same. As the initial concentration of norfloxacin increases, the adsorption capacity increases by the corresponding increase in the probability of contact between the CTAB-ATP/CTS adsorbent and norfloxacin. The adsorption sites per unit dose of CTAB-ATP/CTS are limited. Therefore, when the adsorption sites are occupied, the adsorption of norfloxacin cannot continue, resulting in a decrease in the removal rate of norfloxacin [40].

3.4. Study of CTAB-ATP/CTS Adsorption Mechanism

3.4.1. Adsorption Kinetic Studies

As shown in Figure 4a, when the initial concentrations of norfloxacin were 25 mg/L, 50 mg/L, and 75 mg/L, the adsorption effect of the adsorbent on norfloxacin increased with increasing time, adsorption of norfloxacin by the adsorbent increased rapidly and then stabilised with time, and the adsorption equilibrium of the adsorbent on norfloxacin was essentially achieved at an adsorption time of 240 min, the adsorption capacity was 7.80 mg/g, 15.74 mg/g, and 20.09 mg/g. As the time period progressed, more and more norfloxacin was adsorbed on the surface of CTAB-ATP/CTS, the adsorption gaps decreased, and the adsorption basically equilibrated and gradually reached saturation. This is because at the beginning of adsorption, a large number of empty adsorption sites on the surface of the adsorbent led to initial rapid adsorption, and when almost all external active sites were occupied, the NOR was distributed in the pores and slowly absorbed through the inner surface of the adsorbent.

The fitting results of the Pseudo first kinetic model and Pseudo second kinetic model for the adsorption of norfloxacin by CTAB-ATP/CTS are shown in Figure 4b,c, and the results of parameter fitting are shown in Table 2. The results show that R^2 (0.9999, 0.9998, 0.9999) obtained by fitting the quasi-secondary adsorption rate equations to the adsorption data from CTAB-ATP/CTS for the three norfloxacin concentrations is larger than that obtained by Quasi–Primary equations R^2 (0.9523, 0.9585, 0.9878). In addition, the theoretical equilibrium adsorption amounts (7.8180 mg/g, 15.8153 mg/g, 20.1898 mg/g) obtained from the quasi-primary equation fitting were more consistent with the actual adsorption amounts (7.80 mg/g, 15.74 mg/g) corresponded to 20.09 mg/g), so that the adsorption of CTAB-ATP/CTS corresponded more closely to the quasi-primary model, which suggests some chemisorption in the process [41]. From the fitted model of intraparticle diffusion in Figure 4d, it can be seen that the adsorption of norfloxacin by CTAB-ATP/CTS was divided into three stages, with the first stage curve being steep and corresponding to the stage of extraparticle diffusion; when there was a high concentration of norfloxacin in the solution and due to the concentration difference, norfloxacin diffused into the liquid film outside the adsorbent. The second stage curve was smoother and the NOR diffused from the surface of the adsorbent to the interior of the pores and the adsorption rate decreased. The third stage curve is flat, indicating that the adsorption has reached equilibrium at

this time [42]. Meanwhile, the fitted lines of both stage 1 and stage 2 do not pass through the origin, indicating that both liquid film diffusion and intra-particle diffusion limit the adsorption rate [43,44]. Furthermore, the values of the constant C (reflecting the boundary layer thickness) in stage 2 were higher than those in stage 1 for all adsorption processes with different initial concentrations, suggesting that intraparticle diffusion plays an important role in both rate-determining steps [45].

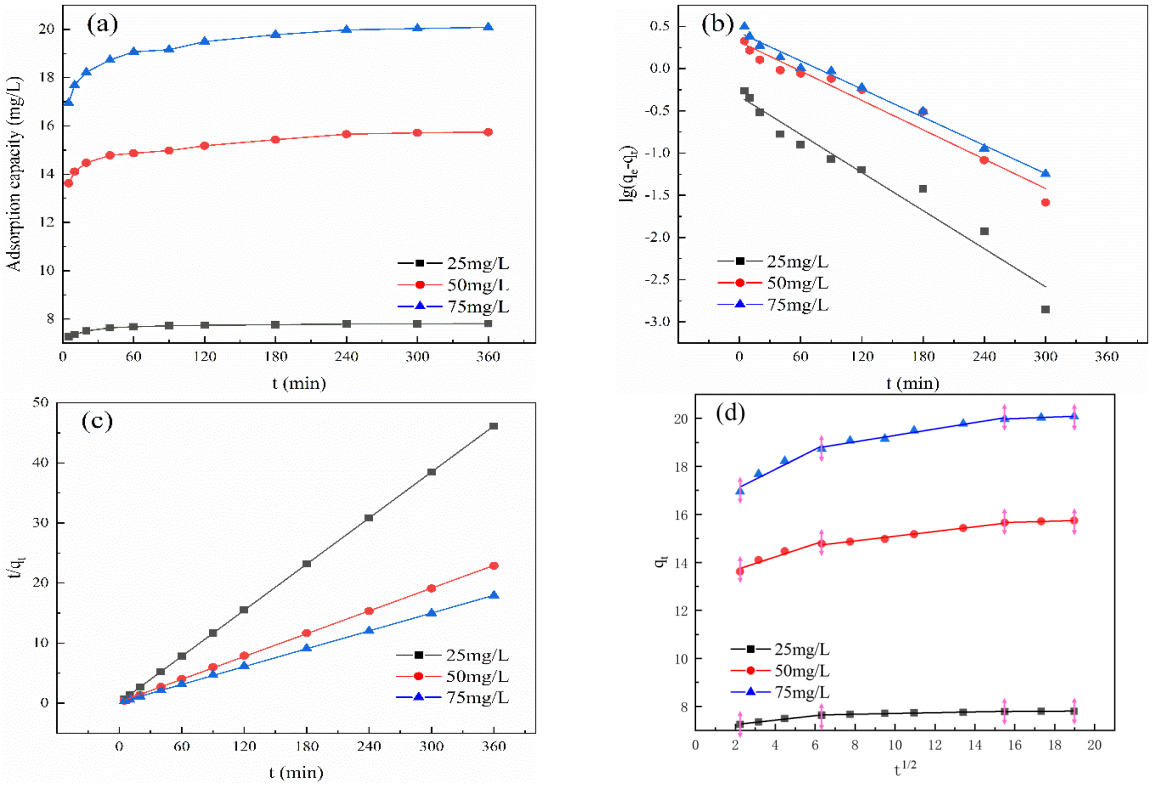

Figure 4. Adsorption kinetic model fitting for adsorption of norfloxacin by CTAB-ATP/CTS: (**a**) adsorption capacity versus time; (**b**) pseudo-first-order kinetic model fitting; (**c**) pseudo-second-order kinetic model fitting; (**d**) intra-particle diffusion model fitting. Note: the arrows show the dividing lines of the three stages.

Table 2. Fitting parameters for adsorption kinetics of norfloxacin by CTAB-ATP/CTS.

Models	Parameters	NOR Initial Concentration		
		25 mg/L	50 mg/L	75 mg/L
pseudo-first-order kinetic	k_1	0.0075	0.0058	0.0056
	q_e	0.4708	2.0839	2.6631
	R^2	0.9523	0.9585	0.9878
pseudo-second-order kinetic	k_1	0.1405	0.0223	0.0178
	q_e	7.8180	15.8153	20.1898
	R^2	0.9999	0.9998	0.9999
intra-particle diffusion	k_1	0.0930	0.2726	0.4178
	C_1	7.0582	13.1400	16.2070
	R_1^2	0.9837	0.9083	0.9168
	k_2	0.0162	0.0982	0.1337
	C_2	7.5469	14.109	17.9550
	R_2^2	0.9430	0.9845	0.9715
	k_3	0.0045	0.0244	0.0324
	C_3	7.7194	15.282	19.4732
	R_3^2	0.9486	0.9485	0.9983

3.4.2. Adsorption Isotherm Studies

The adsorption isotherms of CTAB-ATP/CTS on norfloxacin at different temperatures are shown in Figure 5a. The results showed that the adsorption of norfloxacin by the adsorbent was positively proportional to the adsorption temperature, indicating that warming was favourable for adsorption to proceed.

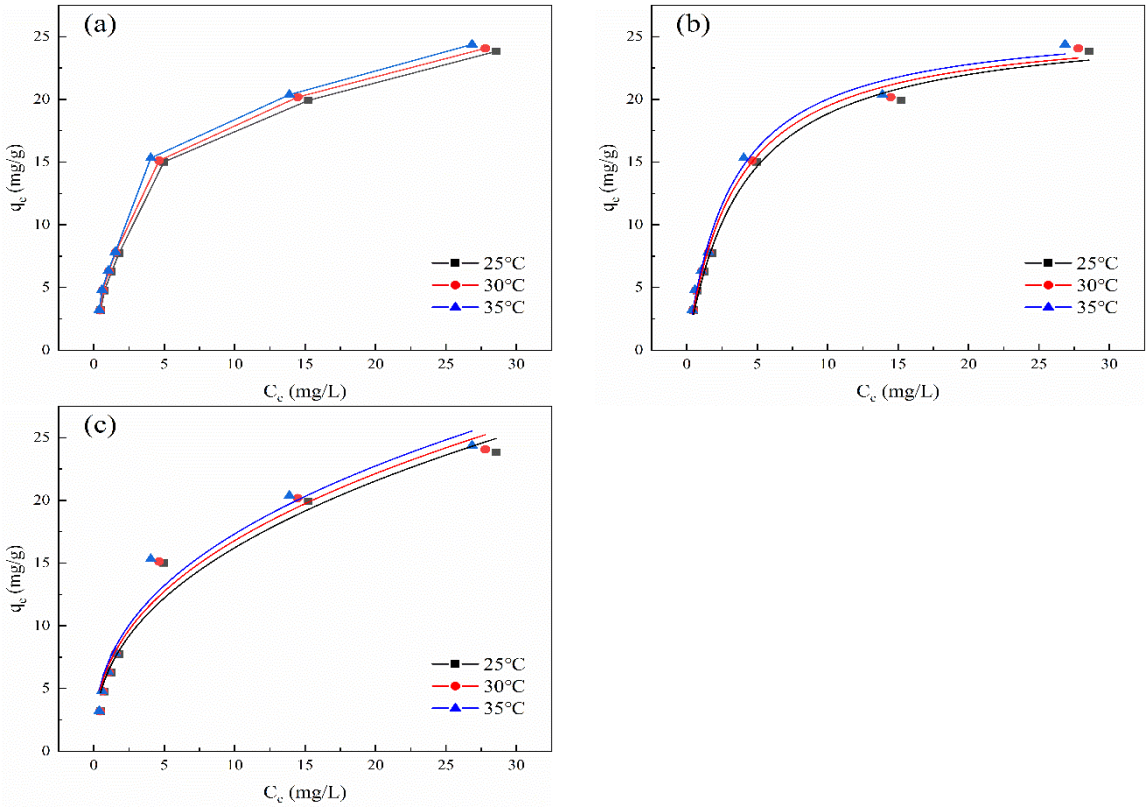

Figure 5. Isothermal adsorption of CTAB-ATP/CTS on norfloxacin at different temperatures fitted to (**a**) the effect of different initial concentrations on the performance of CTAB-ATP/CTS at different temperatures; (**b**) Langmuir isothermal model fitting; and (**c**) Freundlich isothermal model fitting.

The fitting of the adsorption isotherm model of CTAB-ATP/CTS for norfloxacin is shown in Figure 5b,c, and the parameter fitting results are shown in Table 3. The results showed that the adsorption process of CTAB-ATP/CTS for norfloxacin was more consistent with the Langmiur isotherm model, and the correlation coefficients of fitting at different temperatures were higher than the correlation coefficients of the Freundlich model, indicating that the adsorption process represents the homogeneous adsorption of monomolecular layers [46]. Furthermore, 1/n is a measure of surface heterogeneity or exchange strength. The 1/n values of the isothermal Freundlich model were below 0.5 at various temperatures, indicating that the reaction process was relatively easy to carry out (1/n < 0.5, simple; 0.5 < 1/n < 1, not easy; 1/n > 1, very difficult) [47].

Table 3. Fitting parameters for isothermal adsorption of norfloxacin by CTAB-ATP/CTS at different temperatures.

Temperatures	Langmuir Isothermal Model			Freundlich Isothermal Model		
	q_m (mg/g)	K_L	R^2	K_F	$\frac{1}{n}$	R^2
25 °C	26.4300	0.3123	0.9903	7.0197	0.3924	0.9532
30 °C	26.1949	0.2896	0.9935	6.7098	0.3984	0.9596
35 °C	26.3556	0.2511	0.9933	6.3121	0.4098	0.9594

4. Conclusions

In this work, CTAB-ATP/CTS, a natural mineral-based composite adsorbent, was prepared using cetyltrimethylammonium bromide-modified bumpy clay and complexed with chitosan, and its adsorption efficiency of norfloxacin in water was studied. The CTAB-ATP/CTS prepared under the conditions of acetic acid concentration (v/v) of 9%, ultrasonication time of 25 min and CTAB-ATP/CTS composite mass ratio of 1:0.01 showed the best removal and adsorption of norfloxacin, which were 84.79% and 21.20 mg/g, respectively. The original ATP, CTAB-ATP/CTS under optimal preparation conditions, and CTAB-ATP/CTS after adsorption of norfloxacin were compared by SEM, FTIR, XRD, and BET. The results showed that CTAB-ATP/CTS was structurally stable and the specific surface area and total void volume were larger than before modification, which creates more adsorption sites. The removal rate and adsorption capacity of CTAB-ATP/CTS for norfloxacin could be up to 94.62% and 15.77 mg/g under the conditions of initial pH of 7, adsorbent dose of 3 g/L, and initial concentration of 50 mg/L, and was placed in an electrically heated constant temperature oscillating water bath at 25 °C and a speed of 120 rpm for 4 h. The removal and adsorption capacity of CTAB-ATP/CTS adsorption of norfloxacin fit well with the pseudo-second-order kinetic model, and the adsorption process was dominated by chemisorption, with both liquid film diffusion and intraparticle diffusion limiting the adsorption rate. Compared with the Freundlich isothermal model, the adsorption of norfloxacin by CTAB-ATP/CTS was more consistent with the Langmuir isothermal model, indicating that the adsorption process was homogeneous adsorption in the monomolecular layer and that the process was relatively easy to carry out. The adsorbent of CTAB-ATP/CTS was environmentally friendly, safe, efficient, and without secondary pollution, which could provide a new idea for the treatment of antibiotic wastewater.

Supplementary Materials: The following supporting information can be downloaded at: https://www.mdpi.com/article/10.3390/w16172446/s1, Figure S1: Standard curves for norfloxacin: (a) norfloxacin concentration 0-10 mg/L; (b) norfloxacin concentration 0–30 mg/L.

Author Contributions: Conceptualization, H.D., Z.W. and Y.S.; methodology, H.D., Z.W. and Y.S.; validation, H.D., Z.W. and Y.S.; formal analysis, H.D. and Y.S.; investigation, H.D. and Y.S.; resources, Y.S.; data curation, Y.S.; writing—original draft preparation, H.D. and Y.S.; writing—review and editing, Y.S.; visualization, Y.S.; supervision, Y.S. and K.J.S.; project administration, Y.S. and K.J.S.; funding acquisition, Y.S. All authors have read and agreed to the published version of the manuscript.

Funding: This research was supported by the National Natural Science Foundation of China (No. 51508268), the Natural Science Foundation of Jiangsu Province in China (No. BK20201362), and the 2018 Six Talent Peaks Project of Jiangsu Province (JNHB-038).

Data Availability Statement: Data is contained within the article.

Conflicts of Interest: The authors declare no conflict of interest.

References

1. Yang, W.; Lu, Y.; Zheng, F.; Xue, X.; Li, N.; Liu, D. Adsorption behavior and mechanisms of norfloxacin onto porous resins and carbon nanotube. *Chem. Eng. J.* **2012**, *179*, 112–118. [CrossRef]
2. Li, W.; Shi, Y.; Gao, L.; Liu, J.; Cai, Y. Occurrence, distribution and potential affecting factors of antibiotics in sewage sludge of wastewater treatment plants in China. *Sci. Total Environ.* **2013**, *445*, 306–313. [CrossRef]
3. Fang, N.; He, Q.; Sheng, L.; Xi, Y.; Zhang, L.; Liu, H.; Cheng, H. Toward broader applications of iron ore waste in pollution control: Adsorption of norfloxacin. *J. Hazard. Mater.* **2021**, *418*, 126273. [CrossRef] [PubMed]
4. Magureanu, M.; Bilea, F.; Bradu, C.; Hong, D. A review on non-thermal plasma treatment of water contaminated with antibiotics. *J. Hazard. Mater.* **2021**, *417*, 125481. [CrossRef]
5. Yang, H.; Wang, S.; Liu, Y.; Hu, Y.; Shen, W. ZIF-67 grows in chitosan-rGO hydrogel beads for efficient adsorption of tetracycline and norfloxacin. *Sep. Purif. Technol.* **2024**, *330*, 125208. [CrossRef]
6. Wang, L.; Qiang, Z.; Li, Y.; Ben, W. An insight into the removal of fluoroquinolones in activated sludge process: Sorption and biodegradation characteristics. *J. Environ. Sci.* **2017**, *56*, 263–271. [CrossRef]

7. Tong, J.; Chen, L.; Cao, J.; Yang, Z.; Xiong, W.; Jia, M.; Xiang, Y.; Peng, H. Biochar supported magnetic MIL-53-Fe derivatives as an efficient catalyst for peroxydisulfate activation towards antibiotics degradation. *Sep. Purif. Technol.* **2022**, *294*, 121064. [CrossRef]
8. Wu, H.; Niu, X.; Yang, J.; Wang, C.; Lu, M. Retentions of bisphenol A and norfloxacin by three different ultrafiltration membranes in regard to drinking water treatment. *Chem. Eng. J.* **2016**, *294*, 410–416. [CrossRef]
9. Fang, X.; Wu, S.; Wu, Y.; Yang, W.; Li, W.; He, J.; Hong, P.; Nie, M.; Xie, C.; Wu, Z.; et al. High-efficiency adsorption of norfloxacin using octahedral UIO-66-NH_2 nanomaterials: Dynamics, thermodynamics, and mechanisms. *Appl. Surf. Sci.* **2020**, *518*, 146226. [CrossRef]
10. Wang, S.; Yuan, R.; Chen, H.; Wang, F.; Zhou, B. Anaerobic biodegradation of four sulfanilamide antibiotics: Kinetics, pathways and microbiological studies. *J. Hazard. Mater.* **2021**, *416*, 125840. [CrossRef]
11. Ghosh, S.; Kar, S.; Pal, T.; Ghosh, S. Sunlight-driven photocatalytic degradation of Norfloxacin antibiotic in wastewater by ZnSe microsphere functionalized RGO composite. *Sustain. Chem. Environ.* **2023**, *4*, 100038. [CrossRef]
12. Zhang, Y.; Xiao, R.; Wang, S.; Zhu, H.; Song, H.; Chen, G.; Lin, H.; Zhang, J.; Xiong, J. Oxygen vacancy enhancing Fenton-like catalytic oxidation of norfloxacin over prussian blue modified CeO_2: Performance and mechanism. *J. Hazard. Mater.* **2020**, *398*, 122863. [CrossRef]
13. Wang, H.; Cheng, Z.; Zhu, N.; Yuan, H.; Lou, Z.; Otieno, P.; Li, W. pH-dependent norfloxacin degradation by E+-ozonation: Radical reactivities and intermediates identification. *J. Clean. Prod.* **2020**, *265*, 121722. [CrossRef]
14. Ohale, P.; Igwegbe, C.; Iwuozor, K.; Emenike, E.; Obi, C.; Białowiec, A. A review of the adsorption method for norfloxacin reduction from aqueous media. *MethodsX* **2023**, *10*, 102180. [CrossRef] [PubMed]
15. Nasrollahi, N.; Vatanpour, V.; Khataee, A. Removal of antibiotics from wastewaters by membrane technology: Limitations, successes, and future improvements. *Sci. Total Environ.* **2022**, *838*, 156010. [CrossRef] [PubMed]
16. Zhang, X.; Bhattacharya, T.; Wang, C.; Kumar, A.; Nidheesh, P. Straw-derived biochar for the removal of antibiotics from water: Adsorption and degradation mechanisms, recent advancements and challenges. *Environ. Res.* **2023**, *237*, 116998. [CrossRef]
17. Nayak, A.; Bhushan, B.; Kotnala, S. Fabrication of chitosan-hydroxyapatite nano-adsorbent for removal of norfloxacin from water: Isotherm and kinetic studies. *Mater. Today Proc.* **2022**, *61*, 143–149. [CrossRef]
18. Li, J.; Liu, Y.; Wang, J.; Liu, Y.; Zhang, M.; Zhao, L.; Gu, S.; Lin, R.; Chen, L. Research progress on the application of natural adsorbents in the treatment of livestock wastewater. *Desalin. Water Treat.* **2024**, *317*, 100018. [CrossRef]
19. Pan, Z.; Zeng, B.; Shen, L.; Teng, J.; Lai, T.; Zhao, L.; Yu, G.; Lin, H. Innovative Treatment of Industrial Effluents through Combining Ferric Iron and Attapulgite Application. *Chemosphere.* **2024**, *358*, 142132. [CrossRef]
20. Liu, J.; Bai, R.; Zhang, X. Fabrication of the Pesticide-Attapulgite composites regulated by mixed-surfactants. *J. Ind. Eng. Chem.* **2023**, *119*, 461–475. [CrossRef]
21. Wang, H.; Zhang, D.; Zhao, Y.; Xie, M. Cationic surfactant modified attapulgite for removal of phenol from wastewater. *Colloids Surf. A Physicochem. Eng. Asp.* **2022**, *641*, 128479. [CrossRef]
22. Rostamian, M.; Hosseini, H.; Fakhri, V.; Talouki, P.; Farahani, M.; Gharehtzpeh, A.; Goodarzi, V.; Su, C. Introducing a bio sorbent for removal of methylene blue dye based on flexible poly(glycerol sebacate)/chitosan/graphene oxide ecofriendly nanocomposites. *Chemosphere* **2022**, *289*, 133219. [CrossRef]
23. Nayak, A.; Bhushan, B.; Kotnala, S. Evaluation of hydroxyapatite-chitosan-magnetite nanocomposites for separation of pharmaceuticals from water: A mechanistic and comparative approach. *J. Hazard. Mater. Adv.* **2023**, *10*, 100308. [CrossRef]
24. Khan, M.; Abdulhameed, A.; Alshahrani, H.; Algburi, S. Chitosan/functionalized fruit stones as a highly efficient adsorbent biomaterial for adsorption of brilliant green dye: Comprehensive characterization and statistical optimization. *Int. J. Biol. Macromol.* **2024**, *263*, 130465. [CrossRef] [PubMed]
25. Mu, C.; Zhang, L.; Zhang, X.; Zhong, L.; Li, Y. Selective adsorption of Ag (I) from aqueous solutions using Chitosan/polydopamine@C@magnetic fly ash adsorbent beads. *J. Hazard. Mater.* **2020**, *381*, 120943. [CrossRef] [PubMed]
26. Guo, J.; Chen, S.; Liu, L.; Li, B.; Yang, P.; Zhang, L.; Feng, Y. Adsorption of dye from wastewater using chitosan–CTAB modified bentonites. *J. Colloid Interface. Sci.* **2012**, *382*, 61–66. [CrossRef]
27. Zhu, Y.; Zheng, Y.; Wang, A. Preparation of granular hydrogel composite by the redox couple for efficient and fast adsorption of La(III) and Ce(III). *J. Environ. Chem. Eng.* **2015**, *3*, 1416–1425. [CrossRef]
28. Tao, C.; Xu, J.; Shi, S.; Dai, J.; Ji, H. Environmental-friendly nanocomposite attapulgite modified by β-cyclodextrin and ionic liquid for the adsorption of thiamethoxam. *J. Water Process Eng.* **2023**, *53*, 103838. [CrossRef]
29. Shi, W.; Fu, Y.; Jiang, W.; Ye, Y.; Kang, J.; Liu, D.; Ren, Y.; Li, D.; Luo, C.; Xu, Z. Enhanced phosphate removal by zeolite loaded with Mg-Al-La ternary (hydr)oxides from aqueous solutions: Performance and mechanism. *Chem. Eng. J.* **2019**, *357*, 33–44. [CrossRef]
30. Teng, Y.; Jiang, Z.; Yu, A.; Yu, H.; Huang, Z.; Zou, L. Optimization of preparation parameters for environmentally friendly attapulgite functionalized by chitosan and its adsorption properties for Cd^{2+}. *Environ. Sci. Pollut. Res.* **2021**, *28*, 44064–44078. [CrossRef]
31. Liu, Y.; Liu, Y.; Niu, Y.; Qu, R. Fast and highly efficient removal of organic dyes from aqueous solution by attapulgite modified with different amino groups. *Colloids Surf. A Physicochem. Eng. Asp.* **2024**, *687*, 133543. [CrossRef]
32. Kong, H.; Li, Q.; Zheng, X.; Chen, P.; Zhang, G.; Huang, Z. Lanthanum modified chitosan-attapulgite composite for phosphate removal from water: Performance, mechanisms and applicability. *Int. J. Biol. Macromol.* **2023**, *224*, 984–997. [CrossRef]

33. Li, Y.; Wang, Z.; Xie, X.; Zhu, J.; Li, R.; Qin, T. Removal of Norfloxacin from aqueous solution by clay-biochar composite prepared from potato stem and natural attapulgite. *Colloids Surf. A Physicochem. Eng. Asp.* **2017**, *514*, 126–136. [CrossRef]
34. Wu, X.; Huang, M.; Zhou, T.; Mao, J. Recognizing removal of norfloxacin by novel magnetic molecular imprinted chitosan/γ-Fe_2O_3 composites: Selective adsorption mechanisms, practical application and regeneration. *Sep. Purif. Technol.* **2016**, *165*, 92–100. [CrossRef]
35. Yan, B.; Niu, C. Adsorption behavior of norfloxacin and site energy distribution based on the Dubinin-Astakhov isotherm. *Sci. Total Environ.* **2018**, *631–632*, 1525–1533. [CrossRef] [PubMed]
36. Yadav, S.; Asthana, A.; Singh, A.; Chakraborty, R.; Vidya, S.; Singh, A.; Carabineiro, S. Methionine-Functionalized Graphene Oxide/Sodium Alginate Bio-Polymer Nanocomposite Hydrogel Beads: Synthesis, Isotherm and Kinetic Studies for an Adsorptive Removal of Fluoroquinolone Antibiotics. *Nanomaterials* **2021**, *11*, 568. [CrossRef] [PubMed]
37. Tang, J.; Mu, B.; Zheng, M.; Wang, A. One-Step Calcination of the Spent Bleaching Earth for the Efficient Removal of Heavy Metal Ions. *ACS Sustain. Chem. Eng.* **2015**, *3*, 1125–1135. [CrossRef]
38. Tang, J.; Wang, L.; Qin, W.; Qing, Z.; Du, C.; Xiao, S.; Yan, B. High reusability and adsorption capacity of acid washed calcium alginate/chitosan composite hydrogel spheres in the removal of norfloxacin. *Chemosphere* **2023**, *335*, 139048. [CrossRef]
39. El-Ghobashy, M.; Salem, I.; El-Dahrawy, W.; Salem, M. Fabrication of α-MnO_2/Fe-Mn binary oxide nanocomposite as an efficient adsorbent for the removal of methylene blue from wastewater. *J. Mol. Struct.* **2023**, *1272*, 134118. [CrossRef]
40. Sharma, P.; Sharma, M.; Laddha, H.; Gupta, R.; Agarwal, M. Non-toxic and biodegradable κ-carrageenan/ZnO hydrogel for adsorptive removal of norfloxacin: Optimization using response surface methodology. *Int. J. Biol. Macromol.* **2023**, *238*, 124145. [CrossRef]
41. Jang, H.; Yoo, S.; Choi, Y.; Park, S.; Kan, E. Adsorption isotherm, kinetic modeling and mechanism of tetracycline on Pinus taeda-derived activated biochar. *Bioresour. Technol.* **2018**, *259*, 24–31. [CrossRef] [PubMed]
42. Teng, R.; Shi, D.; Pan, Y.; Jiang, J.; Song, H.; Tan, W. Synthesis of mesoporous MIL-100(Fe) from acid mine drainage sludge for norfloxacin removal: Industrial sludge high value utilization, adsorbent performance and contaminant removal mechanisms. *Colloids Surf. A Physicochem. Eng. Asp.* **2024**, *684*, 133032. [CrossRef]
43. Xie, R.; Zhou, L.; Smith, A.; Almquist, C.; Berberich, J.; Danielson, N. dual grafted fluorinated hydrocarbon amine weak anion exchange resin polymer for adsorption of perfluorooctanoic acid from water. *J. Hazard. Mater.* **2022**, *431*, 128521. [CrossRef]
44. Tan, L.; Yu, J.; Pang, Y.; Zeng, G.; Deng, Y.; Wang, J.; Ren, X.; Ye, S.; Peng, B.; Feng, H. Sustainable efficient adsorbent: Alkali-acid modified magnetic biochar derived from sewage sludge for aqueous organic contaminant removal. *Chem. Eng. J.* **2018**, *336*, 160–169.
45. Ma, Y.; Wu, L.; Li, P.; Yang, L.; He, L.; Chen, S.; Yang, Y.; Gao, F.; Qi, X.; Zhang, Z. A novel, efficient and sustainable magnetic sludge biochar modified by graphene oxide for environmental concentration imidacloprid removal. *J. Hazard. Mater.* **2020**, *407*, 124777. [CrossRef] [PubMed]
46. Cheng, T.; Zhang, Y.; Cui, F.; Jiang, G.; Liu, P.; Guo, J.; Cui, K.; Chen, C.; Li, H. Preparation of novel ZIF-8 aerogel adsorbent based on cellulose and the application of Cu (II) removal from wastewater. *Chem. Phys. Lett.* **2022**, *808*, 140100. [CrossRef]
47. Wang, Y.; Yu, S.; Yuan, H.; Zhang, L. Constructing N,S co-doped network biochar confined $CoFe_2O_4$ magnetic nanoparticles adsorbent: Insights into the synergistic and competitive adsorption of Pb^{2+} and ciprofloxacin. *Environ. Pollut.* **2024**, *343*, 123178. [CrossRef]